Sensors and Actuators A 315 (2020) 112247

Contents lists available at ScienceDirect

Sensors and Actuators A: Physical

journal homepage: www.elsevier.com/locate/sna

Single digit parts-per-billion NO_x detection using MoS_2/hBN transistors

Ayaz Ali [a,b], Ozhan Koybasi [c], Wen Xing [d], Daniel N. Wright [c], Deepak Varandani [e], Takashi Taniguchi [f], Kenji Watanabe [f], Bodh R. Mehta [e], Branson D. Belle [a,d,*]

[a] Department of Smart Sensor Systems, SINTEF DIGITAL, Oslo, 0373, Norway
[b] Department of Electronic Engineering, University of Sindh, Jamshoro, 76080, Pakistan
[c] Department of Microsystems and Nanotechnology, SINTEF DIGITAL, Oslo, 0373, Norway
[d] Department of Sustainable Energy Technology, SINTEF INDUSTRY, Oslo, 0373, Norway
[e] Department of Physics, Indian Institute of Technology Delhi, Delhi-110016, India
[f] National Institute for Materials Science (NIMS), Tsukuba, Ibaraki, 305-0044, Japan

ARTICLE INFO

Article history:
Received 20 April 2020
Received in revised form 14 July 2020
Accepted 31 July 2020
Available online 6 August 2020

Keywords:
Molybdenum disulphide (MoS_2)
Field effect transistor (FET)
Gas sensor
NO_x detection
Sensitivity

ABSTRACT

2D materials offer excellent possibilities for high performance gas detection due to their high surface-to-volume ratio, high surface activities, tunable electronic properties and dramatic change in resistivity upon molecular adsorption. This paper demonstrates a simple field effect transistor (FET) of molybdenum disulphide (MoS_2) fabricated on a hexagonal boron nitride (hBN) substrate that can detect NO_x down to concentrations of 6 ppb and possibly far below at room temperature (RT) with a systematic optimization of the device design and fabrication parameters as well as the device operating conditions. The effects of the substrate, number of MoS_2 layers, channel layout and biasing conditions on the response of MoS_2 FETs to NO_x were investigated, providing directions for maximizing the sensitivity. This work also sheds light the issues of recovery and stability and present a methodology for calibration of the sensors which is critical for repeatable and reliable measurements.

1. Introduction

Industrialization and urbanization worldwide has led to increased levels of air-pollutants which can seriously negatively impact human health as well as increase global environment hazards such as ozone layer deterioration, acid rain and photochemical smog [1,2]. These air-pollutants mainly contain harmful gasses such as carbon monoxide (CO), nitrogen oxides (NO_x) or sulphur dioxide (SO_2). It has been noted that an exposure to NO_x concentrations even as low as 53 parts-per-billion (ppb) can potentially damage the human respiration system [3–6]. Existing technology to detect these hazardous gases is based on metal oxides which requires high operating temperatures (> 200 °C) to activate the gas sensing processes (adsorption/desorption), which not only requires fabrication complexity but also leads to high power consumption [7–9].

Conversely, two-dimensional (2D) materials have emerged as a very promising class of materials which have been used to develop ultrahigh sensitive and low-power-consumption gas sensors due to their unmatched surface area per unit volume, high surface activities and unique electronic properties [10–14]. Graphene based gas sensors have shown remarkable performance by sensing down to a single gas molecule at room temperature [15]. For high performance gas sensors, transition metal dichalcogenides (TMDs) offer a route to obtain semiconducting properties which is a key parameter, unlike graphene which has a zero bandgap [16–18].

Recent works on MoS_2 based NO_x sensors have demonstrated the potential of this class of materials with excellent sensitivities ranging from 100 ppm to 8 ppb [19–31]. In these works, elevated temperature, nanoparticles, and red light have been used, which increases the power consumption and complexity and added steps in device fabrication. Given that the United States Environmental Protection agency has stipulated 53 ppb of NO_x as being dangerous [6], it is imperative to develop low cost highly sensitive NO_x sensors.

It is known that devices that employ hBN as a substrate are robust and have increased performance due to the reduction of electron-hole puddles and scattering sites given the atomically flat surface [32–34]. In this paper, we employ high quality hBN

* Corresponding author at: Department of Smart Sensor Systems, SINTEF DIGITAL, Oslo, 0373, Norway.
E-mail address: Branson.Belle@sintef.no (B.D. Belle).

https://doi.org/10.1016/j.sna.2020.112247

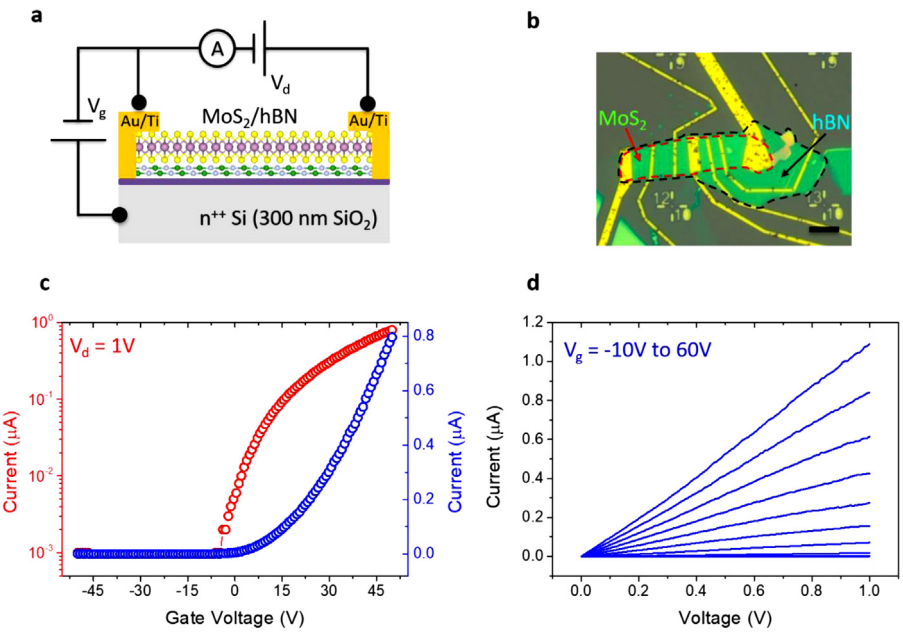

Fig. 1. Schematic and optical image (scale bar 10 μm) of single layer MoS_2/hBN transistor (a,b). MoS_2/hBN transistor characteristics (c,d). (c) Transfer characteristics at drain voltage (V_d) of 1 V. (d) series of output characteristic curves with different gate voltages (V_g = −10 V to 60 V).

as a substrate for our mechanically exfoliated MoS_2 devices and demonstrate sensitivity down to at least 6 ppb for NO_x detection at room temperature through a systematic optimization of the device parameters and operating conditions. Our work provides significant information on the impact of various structural parameters such as type of substrate, number of MoS_2 layers and channel geometry on the response. Moreover, we discuss in detail the sensor biasing conditions and their adjustment to obtain consistent and reliable measurement results as well as maximal sensitivity.

2. Experimental methods

2.1. Device fabrication

The MoS_2/hBN Van der Waals heterostructures were fabricated by a dry transfer technique using mechanically exfoliated flakes [35] (details in supporting information Fig. S1). Electron-beam lithography (EBL) was used to pattern the MoS_2 channel with subsequent shaping via reactive ion etching using a mixture of CHF_4 and O_2 gases. Finally, electrodes were realized by EBL and e-beam evaporation and lift-off of Ti/Au (5 nm/100 nm) metals.

2.2. Raman characterization

Raman characterization was carried out using a MonoVista CRS + system with 532 nm laser. The laser power was sufficiently low to avoid sample damage. Additionally, Raman characterization was performed on flake of similar thickness not within the channel of the device.

2.3. Gas measurements

Gas measurements were carried out in a custom gas chamber at atmospheric pressure. The NO_x used was a 50/50 mixture of NO_2 and NO. Pre-diluted NO_x gas bottles were purchased from Linde Gas AS (Norway) with concentration of 50 and 5 ppm balanced by argon. For obtaining desired gas concentration in this work, the gases were further diluted by mixing with argon before supplying to the gas chamber. The total flow rate of the gases was between 40–80 ml/min.

3. Results and discussions

A single layer MoS_2/hBN field effect transistor (FET) with a channel length of 7 μm and channel width of 10 μm was used as the reference device structure for our work (Fig. 1(a)). The Raman measurement data confirming single-layer thickness of the MoS_2 channel is included in supporting information Fig. S2. An optical image of the device is shown in Fig. 1(b). Fig. 1(c,d) shows the transfer and output characteristics of the fabricated reference device,

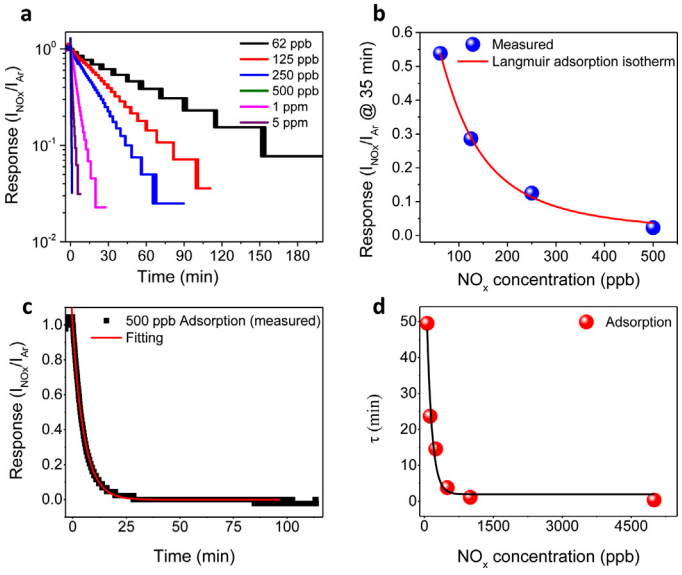

Fig. 2. Sensor response under the different NO_x exposures at zero gate voltage (V_g = 0 V) (a) and NO_x gas response at fixed time (35 min) for different gas concentrations (62, 125, 250 and 500 ppb) (b). Time dependent response change under the NO_x exposure of 500 ppb and the corresponding fitted curve using the exponential decay function (c) and extracted adsorption rate constant (τ) from curve fitting for different NO_x concentrations (d).

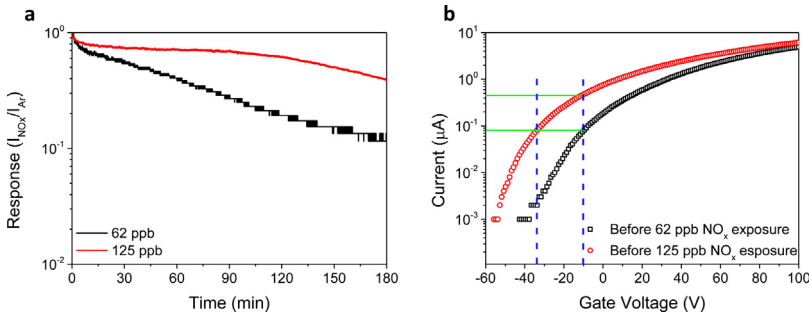

Fig. 3. Sensor response under the two different NO_x exposures (62 ppb and 125 ppb) at -10 V gate voltage (a), measured transfer characteristics curves prior to each gas measurements (b).

which was operated in two terminal configuration. As seen in Fig. 1, the device shows n-type behaviour where drain current increases with increasing gate voltage. The field effect mobility extracted from the transfer characteristics is 1.16 $cm^2\ V^{-1}\ s^{-1}$.

Fig. 2(a) shows the normalized responses of the device to different concentrations of NO_x ranging from 5000 ppb down to 62 ppb at a gate voltage of 0 V. The gas response is normalized as $I_{NOx}/\ I_{Ar,}$ where I_{NOx} and I_{Ar} refer to drain current during the NO_x exposure and prior to NO_x in Ar atmosphere, respectively. Upon exposure to NO_x, the drain current decreases and threshold voltage (V_{th}) shifts toward positive gate voltages, indicating p-type doping of the channel with NO_x exposure. These attributes confirm that the gas sensing process is based on charge transfer mechanism, where NO_x captures electrons from the MoS_2 channel. As the concentration of NO_x increases, more charges per unit time are transferred from MoS_2 to NO_x, leading to a steeper decrease in the drain current (Fig. 2(a)). Fig. 2(b) shows that our device exhibits good response, capable of detecting very low concentrations of NO_x (62 ppb) at room temperature and follows the Langmuir isotherm for molecules adsorbed on the surface (Fig. 2(b)). It therefore confirms that charge transfer is the sensing mechanism [36]. The results also show that the response time is much shorter for higher NO_x concentration (20 s for 5 ppm) as shown in Fig. 2(a) and Fig. S4. Furthermore, the adsorption rate constant (τ) of our sensor was extracted which reveals the rate of the NO_x adsorption process on the MoS_2 surface. Fig. 2(c) illustrates the drain current decreases associated with NO_x adsorption. The data is fitted with an exponential decay function which confirms that there is only one mechanism associated with NO_x adsorption [37]. The adsorption rate constant as the function of different NO_x concentrations is presented in Fig. 2(d). It is observed that τ decreases as the NO_x concentration increases and saturates for the higher NO_x concentrations.

Throughout the rest of the paper, the effects of the device operating conditions and device structure parameters on the response of the device to NO_x were systematically investigated. This study will provide an insight into optimizing these parameters to achieve maximal response to NO_x and sensor calibration methods in order to obtain consistent and reliable measurement results.

3.1. Threshold shift, recovery and gate voltage dependence of the response

As mentioned above, NO_x exposure leads to a significant shift of the device's threshold voltage toward positive gate voltages. Various techniques can be employed to recover MoS_2 gas sensors after NO_x exposure. One method is by applying a negative gate voltage pulse to refresh the sensor [38]. The other methods that can be used to recover the sensor after NO_x exposure are to anneal at elevated temperatures (100–200 °C) [39–41] or light illumination, where photogenerated holes react with adsorbed gas molecules and give rise to desorption [42]. The recovery time of the sensor strongly depends on the intensity of the light. Sensor recovery at room temperature by illuminating with white light from a light emitting diode (LED) was demonstrated which shifts the threshold back to original state (Fig. S3). This room temperature sensor recovery suggests that physisorption of NO_x molecules on mechanically exfoliated MoS_2 is the more dominant. In addition, the cyclic test of sensor response and recovery shows good repeatability as shown in supporting information Fig. S4. In addition to gas exposure, environmental effects such as humidity/water molecules could also shift the sensor's threshold voltage [43,44]. A proper calibration of the sensor after each measurement is therefore essential for repeatability and reliability of the measurement results. The following experiment was conducted to study the consequences of uncalibrated operation. We first measured the gate characteristics and then response of the sensor to a NO_x concentration of 62 ppb at a gate voltage of -10 V. After this measurement, we recovered the sensor using white LED which shifted the threshold voltage back to the original state. Next, the sensor was kept in ambient air for a few days and then the gate characteristics of the sensor was measured again. This was immediately followed by the measurement of the sensor response to a NO_x concentration of 125 ppb at the same gate voltage of -10 V. As can be seen from the results presented in Fig. 3, the device shows lower response to a concentration of 125 ppb as compared to a concentration of 62 ppb. Lower response to higher concentration is attributed to the threshold shift due to environmental effects before the measurement at a concentration of 125 ppb. This is evident from the transfer characteristics measured right before each gas exposure (Fig. 3(b)). The transfer curve had shifted by −25 V before exposure to 125 ppb of NO_x. This shows that by operating the sensor at the same gate voltage of -10 V during the measurement of the response to 125 ppb of NO_x, the device is no longer in the same condition that it was when measuring the response to 62 ppb. To restore the same operating conditions as the first measurement with the gate at -10 V, the device must be operated with the gate at −35 V during the second measurement.

To study the effect of gate voltage on the sensor response and explore the optimum operating conditions, we measured the response of the reference device to NO_x at three different gate voltages. As indicated in Fig. 4, each of the chosen gate voltages corresponds to a different region of the transfer characteristics curve (*i.e.,* regions of different transconductances): *i)* subthreshold region (V_1), *ii)* transition from subthreshold to linear or quadratic region (V_2), and *iii)* linear region (V_3). Due to the threshold shift, the values of V_1, V_2, and V_3 are calibrated before each measurement to ensure that the device is operated at the same condition, i.e., the same doping level. Fig. 5 shows the gate voltage dependence of the response to different concentrations of NO_x. The results show that the maximal sensitivity is achieved when the sensor is operated in the subthreshold region (V_1). This is because at subthreshold regime, the device is depleted of charge carriers and hence the drain

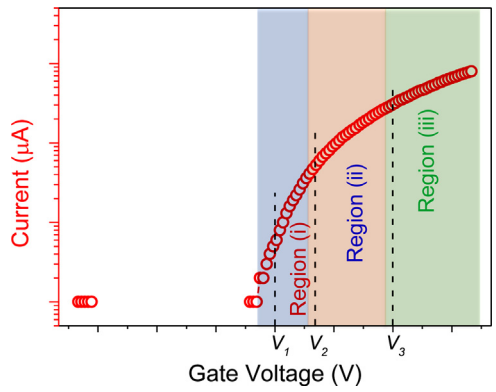

Fig. 4. Transfer characteristic curve in logarithmic scale showing different regions (i) subthreshold (V_1), ii) subthreshold to linear (V_2), and iii) linear (V_3)).

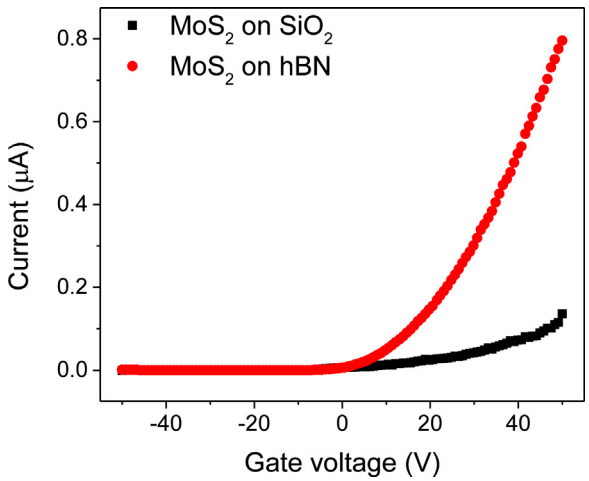

Fig. 6. Transfer characteristic curve of single layer MoS_2/SiO_2 (black curve) and single layer MoS_2/hBN transistor (red curve), respectively. (For interpretation of the references to colour in this figure legend, the reader is referred to the web version of this article).

current changes more abruptly upon exposure to a given concentration of NO_x molecules. However, when the sensor is exposed to the high concentrations of NO_x (5000 ppb), the effect of the gate voltage becomes negligible. Our experimental results are in agreement with the simulation work presented by Rao *et al.* [17]

3.2. *Effect of the substrate*

To study the effect of the substrate on the performance of the gas sensor, a single layer MoS_2 transistor on bare SiO_2 (MoS_2/SiO_2) was fabricated and compared with the reference device which is on hBN (MoS_2/hBN). Fig. S5 in the supporting information shows the optical image of the single layer MoS_2 transistor fabricated on SiO_2 substrate. Before conducting sensing comparison, the transistor performance comparison of these devices was carried out. For effective comparison, both devices were chosen with the same dimensions (channel length and width). The transfer characteristic curves of both devices are presented in Fig. 6. The field effect mobility of the devices was extracted as 1.16 $cm^2\ V^{-1}s^{-1}$ for MoS_2/hBN and 0.25 $cm^2\ V^{-1}s^{-1}$ for MoS_2/SiO_2 transistor, respectively. In addition, the current on/off ratio of 10^4 and 10^3 was observed for MoS_2/hBN and MoS_2/SiO_2 device, respectively. This performance difference can be attributed to fewer interface traps between MoS_2 and hBN compared to MoS_2 and SiO_2. In addition, hBN is an atomically flat substrate with fewer scattering sites.

For the comparison of NO_x gas sensing, both transistors (MoS_2/hBN and MoS_2/SiO_2) were operated in the subthreshold region (Fig. 4), and their responses were measured. Fig. 7 shows that upon exposure to lower concentrations of NO_x (25 ppb), the MoS_2/hBN device exhibits higher response as compared to the MoS_2/SiO_2 device. However, the effect of substrate becomes negli-

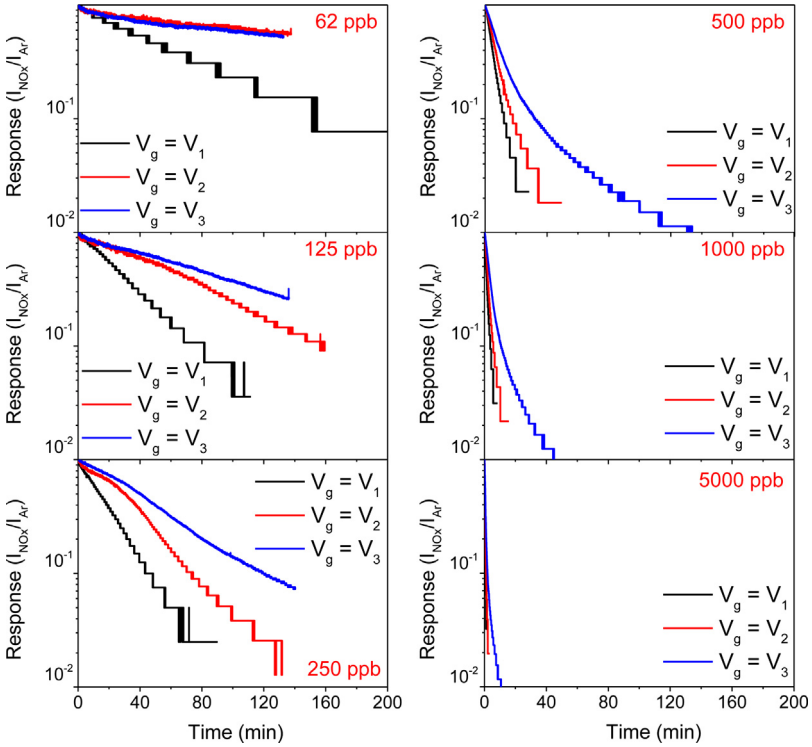

Fig. 5. Gate voltage dependent response of the single layer MoS_2/hBN gas sensor. The sensor was operated at three different gate voltages (V_1, V_2 and V_3) and the response to various NO_x exposures (62, 125, 250, 500, 1000 and 5000 ppb) was measured.

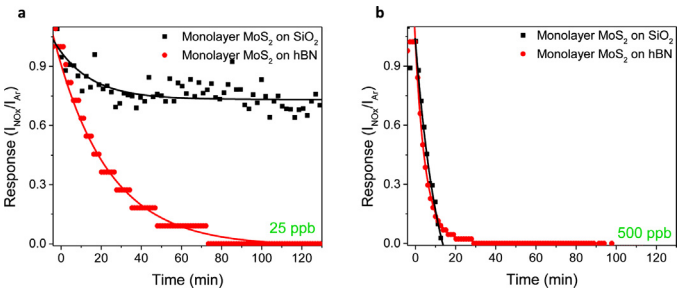

Fig. 7. Effect of the substrate on sensor response. Gas sensing response of MoS_2/SiO_2 and MoS_2/hBN devices under various NO_x exposures (25 and 500 ppb). The sensors were operated at subthreshold gate voltages.

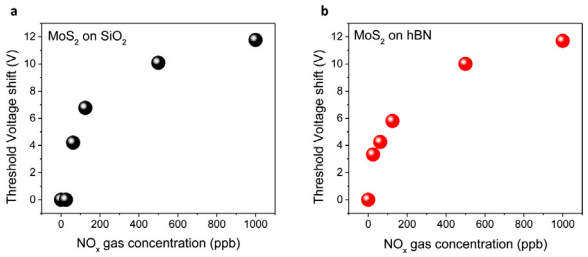

Fig. 8. Threshold voltage shift upon different gas exposures for MoS_2/SiO_2 device (a) and for MoS_2/hBN device (b), respectively.

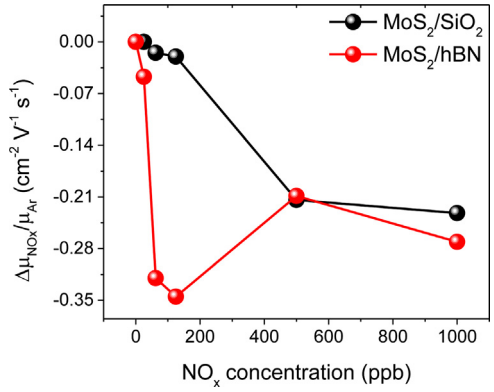

Fig. 9. Effective mobility change as a function of NO_x concentrations (25, 62, 125, 500 and 1000 ppb) for MoS_2/SiO_2 device (black curve) and MoS_2/hBN device (red curve). (For interpretation of the references to colour in this figure legend, the reader is referred to the web version of this article).

gible when the device is exposed to the higher NO_x concentrations (500 ppb).

To understand the mechanism behind the substrate effect, transfer characteristic curves were recorded after each gas measurement and the corresponding threshold voltage shift and change in the mobility for the MoS_2/SiO_2 device and MoS_2/hBN device were extracted and shown in Figs. 8 & 9 . A relatively large threshold voltage shift is observed for the MoS_2/hBN device at low NO_x concentrations (25 ppb) while for higher NO_x concentration, almost same threshold voltage shift is observed for both devices. The threshold voltage shift reflects the amount of charge transfer upon gas exposure; hence, it suggests that the MoS_2/hBN device is more sensitive to ultra-low concentrations of NO_x (25 ppb). Furthermore, a change in mobility is also observed for both devices under NO_x exposure (Fig. 9). In the case of MoS_2/hBN, a sharp decrease in the mobility is observed for low concentration gas exposures. This can be explained by the increase in scattering sites on adsorption of NO_x molecules due to device being more homogeneous on a flatter substrate. However, in case of the MoS_2/SiO_2 device, the change

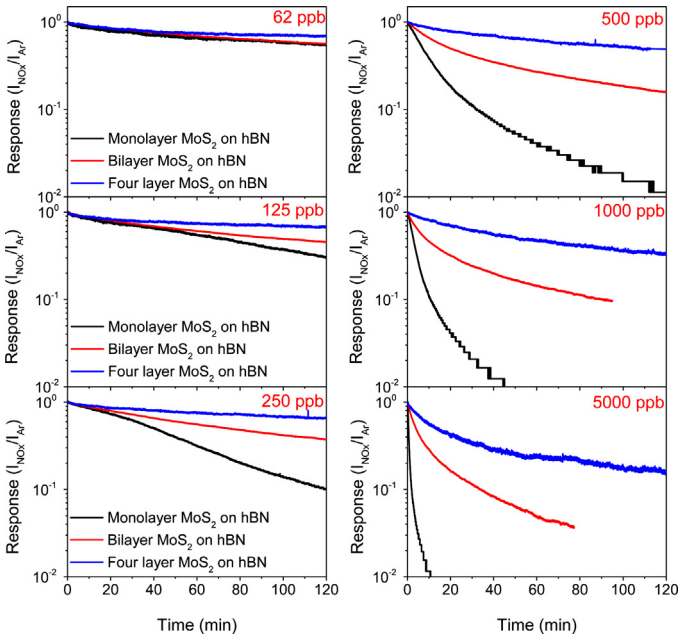

Fig. 10. Effect of the MoS_2 layer thickness on sensor response. Gas sensing response of monolayer, bilayer and four-layer MoS_2 devices under various NO_x exposures (62, 125, 250, 500, 1000 and 5000 ppb). The sensors were operated at saturated regime (V_g = 30 V) in order to keep the doping level same.

in mobility in the presence of NO_x is much lower for low concentrations which shows that effect of surface roughness is more dominant. This can be seen from the pristine device characteristics (Fig. 6), where the MoS_2/hBN device exhibits high mobility and current on/off ratio as compare to MoS_2/SiO_2.

3.3. *Effect of number of layers*

The effect of MoS_2 layer thickness on the response of the sensor to NO_x was also studied. In addition to the reference device, we also fabricated FETs with bilayer and four-layer MoS_2 on hBN. The transfer characteristics curves of the devices with different number of MoS_2 layers are shown in fig. S6. The threshold voltage is different for FETs with different number of MoS_2 layers as the carrier concentration varies with MoS_2 thickness. Hence, operating the devices at same gate voltage would not provide a correct comparison of their response to NO_x. Instead, the devices were operated at different gate voltages that lead to the same doping level or the same effective point of operation on the transfer characteristics curve as discussed in Section 3.1. we operated all three sensors at the linear regime of the transfer characteristics curve (V_g = 30 V) and measured the response of the devices under various NO_x gas exposures as shown in Fig. 10. Our results show that the response decreases with increasing number of MoS_2 layers. This can be attributed to the screening effect [45]. In monolayer MoS_2 FET, NO_x interacts with the surface charge carriers as the channel is monolayer. In the case of multi-layer MoS_2, on the other hand, NO_x interacts less with carriers further away from the top layer. Furthermore, as can be seen in Fig. 10, the effect of number of MoS_2 layers becomes more significant at higher gas concentrations where the response differs by orders of magnitude.

3.4. *Effect of channel dimensions*

To demonstrate the effect of MoS_2 channel dimensions on response, we fabricated hall bar shaped channel (Fig. S7). For comparison, we used two different channel lengths (CHL1 = 12 μm and CHL2 = 24 μm) with same channel width (4 μm) and measured the

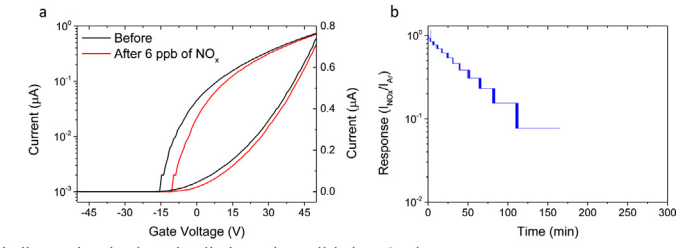

Fig. 11. Sensing of a single digit ppb of NO_x. Transfer characteristic curve of single layer MoS_2/hBN device before and after of an ultra-low exposure of NO_x (6 ppb) (a). Time response of single layer MoS_2/hBN device under an ultra-low exposure of NO_x (6 ppb) (b). The sensor was operated at sub-threshold gate voltage of −5 V.

electrical characteristics for each channel length in order to choose the same operating conditions for the devices. The transfer curves of both channel lengths show the same threshold voltage (Fig. S8), and therefore operating the sensors at same gate voltage gives a correct comparison. Fig. S9 shows the response of the devices with CHL1 and CHL2 under fixed gate bias of -10 V to various NO_x gas concentrations (62, 125, 250, 500, 1000 and 5000 ppb). The device with shorter channel length (CHL1) shows a relatively higher response as compared to long channel (CHL2). This is expected as the charges undergo less scattering during transport through a shorter channel.

3.5. Maximal sensitivity

The results obtained from the above studies allowed us to choose the best parameters for maximum sensitivity. We have demonstrated that higher sensitivities to NO_x can be achieved with monolayer MoS_2 on hBN substrate with short channel length and by operating at the subthreshold regime. By implementing all optimizations based on studies reported in the previous sections, single digit ppb sensitivity to NO_x was obtained. Fig. 11(a) shows the transfer characteristics before and after the exposure of the optimized sensor to 6 ppb of NO_x. A significant shift in the transfer curve was observed even after such low exposures. Moreover, one order of magnitude change in the resistance of MoS_2 was observed within two hours of ultra-low NO_x exposure (6 ppb) as shown Fig. 11(b). The signal to noise ratio is one the important parameters for the high-performance gas sensor, especially for low concentration gas sensors. Our sensor shows an order of magnitude change in resistance at ultra-low exposure (6 ppb). Our experimental setup is currently not capable of providing gas concentrations below 6 ppb, and hence we were not able to explore the ultimate NO_x detection limit of MoS_2 transistors. However, the remarkable response to 6 ppb of NO_x indicates that the detection limit can be well-below 6 ppb.

4. Conclusion and outlook

We performed a comprehensive study on the response of MoS_2 transistors to NO_x exposure. In this study, we demonstrated how the device structure parameters and operating conditions impact the response. Our findings show that the response of the MoS_2 transistors to NO_x can be significantly enhanced by using hBN substrate instead of SiO_2, using monolayer MoS_2 channel, and reducing the channel length. The bias voltage used for the sensor operation also significantly affects the response and our results show that the maximal response is obtained when the device is operated in the subthreshold regime of the transfer characteristics curve. A known characteristic of MoS_2 transistors as gas sensor is their poor self-recovery at room temperature, which was also observed in our work. We have shown that it is extremely important to calibrate the device by adjusting the bias voltage before each operation in order to assure that the measurement results are consistent and reliable. We have demonstrated that MoS_2/hBN transistors with a careful optimization can detect NO_x concentrations as low as 6 ppb (or possibly even significantly lower, which we are not capable of testing due to our experimental setup constraints).

This work was focused on demonstrating ultra-high sensitivity of bare MoS_2/hBN transistor to NO_x at room temperature. We also addressed the issue of recovery. There are also other key parameters that need to be considered for the development of high-performance NO_x sensor such as selectivity, which is beyond the scope of this paper. One method to enhance selectivity to certain gas species is to decorate the MoS_2 transistors with nanoparticles of specific work functions which is currently under investigation by our group.

CRediT authorship contribution statement

Ayaz Ali: Conceptualization, Methodology, Investigation, Writing - original draft, Writing - review & editing, Visualization. **Ozhan Koybasi:** Conceptualization, Methodology, Validation, Writing - review & editing, Supervision. **Wen Xing:** Methodology, Investigation, Resources. **Daniel N. Wright:** Methodology, Investigation, Resources. **Deepak Varandani:** Project administration, Funding acquisition. **Takashi Taniguchi:** Methodology, Resources, Writing - original draft. **Kenji Watanabe:** Methodology, Resources, Writing - original draft. **Bodh R. Mehta:** Conceptualization, Methodology, Writing - review & editing, Supervision, Funding acquisition. **Branson D. Belle:** Conceptualization, Methodology, Validation, Writing - review & editing, Supervision, Funding acquisition.

Declaration of Competing Interest

The authors declare that they have no known competing financial interests or personal relationships that could have appeared to influence the work reported in this paper.

Acknowledgements

This work was supported by the Research Council of Norway (Project no. 280788). The Research Council of Norway is also acknowledged for the support to the Norwegian Micro- and Nano-Fabrication Facility, NorFab, project number 245963/F50. Growth of hexagonal boron nitride crystals was supported by the MEXT Element Strategy Initiative to Form Core Research Center, Grant Number JPMXP0112101001 and the CREST(JPMJCR15F3), JST.

Appendix A. Supplementary data

Supplementary material related to this article can be found, in the online version, at doi:https://doi.org/10.1016/j.sna.2020.112247.

References

[1] S. Gulia, S.M.S. Nagendra, M. Khare, I. Khanna, Urban air quality management-a review, Atmos. Pollut. Res. 6 (2015) 286–304.
[2] P. Kumar, M. Khare, R.M. Harrison, W.J. Bloss, A.C. Lewis, H. Coe, et al., New directions: air pollution challenges for developing megacities like Delhi, Atmos. Environ. 122 (2015) 657–661.
[3] S.-K. Liu, S. Cai, Y. Chen, B. Xiao, P. Chen, X.-D. Xiang, The effect of pollutional haze on pulmonary function, J. Thorac. Dis. 8 (2016) E41–E56.
[4] M. Guarnieri, J.R. Balmes, Outdoor air pollution and asthma, Lancet 383 (2014) 1581–1592.
[5] K. Wetchakun, T. Samerjai, N. Tamaekong, C. Liewhiran, C. Siriwong, V. Kruefu, et al., Semiconducting metal oxides as sensors for environmentally hazardous gases, Sensors Actuators B: Chem 160 (2011) 580–591.
[6] US Environmental Protection Agency Air Trends Summary Reports; https://www3epagov/ttn/naaqs/standards/nox/s_nox_historyhtml#3.

[7] N. Barsan, D. Koziej, U. Weimar, Metal oxide-based gas sensor research: how to? Sensors Actuators B: Chem 121 (2007) 18–35.
[8] C.-O. Park, S. Akbar, Ceramics for chemical sensing, J. Mater. Sci. 38 (2003) 4611–4637.
[9] G. Korotcenkov, B.K. Cho, Instability of metal oxide-based conductometric gas sensors and approaches to stability improvement (short survey), Sensors Actuators B: Chem 156 (2011) 527–538.
[10] K. Lee, R. Gatensby, N. McEvoy, T. Hallam, G.S. Duesberg, High-performance sensors based on molybdenum disulfide thin films, Adv Mater 25 (2013) 6699–6702.
[11] X. Liu, T. Ma, N. Pinna, J. Zhang, Two-dimensional nanostructured materials for gas sensing, Adv. Funct. Mater. 27 (2017), 1702168.
[12] Y.H. Kim, S.J. Kim, Y.-J. Kim, Y.-S. Shim, S.Y. Kim, B.H. Hong, et al., Self-activated transparent all-graphene gas sensor with endurance to humidity and mechanical bending, ACS Nano 9 (2015) 10453–10460.
[13] Y.H. Kim, J.S. Park, Y.-R. Choi, S.Y. Park, S.Y. Lee, W. Sohn, et al., Chemically fluorinated graphene oxide for room temperature ammonia detection at ppb levels, J. Mater. Chem. A Mater. Energy Sustain. 5 (2017) 19116–19125.
[14] K. Shehzad, T. Shi, A. Qadir, X. Wan, H. Guo, A. Ali, et al., Designing an efficient multimode environmental sensor based on graphene–silicon heterojunction, Int. J. Adv. Mater. Technol. 2 (2017), 1600262.
[15] F. Schedin, A.K. Geim, S.V. Morozov, E.W. Hill, P. Blake, M. Katsnelson, et al., Detection of individual gas molecules adsorbed on graphene, Nat. Mater. 6 (2007) 652–655.
[16] Z. Feng, Y. Xie, J. Chen, Y. Yu, S. Zheng, R. Zhang, et al., Highly sensitive $MoTe_2$ chemical sensor with fast recovery rate through gate biasing, 2d Mater. 4 (2017), 025018.
[17] D.J. Late, Y.-K. Huang, B. Liu, J. Acharya, S.N. Shirodkar, J. Luo, et al., Sensing behavior of atomically thin-layered MoS_2 transistors, ACS Nano 7 (2013) 4879–4891.
[18] B. Liu, L. Chen, G. Liu, A.N. Abbas, M. Fathi, C. Zhou, High-performance chemical sensing using Schottky-contacted chemical vapor deposition grown monolayer MoS_2 transistors, ACS Nano 8 (2014) 5304–5314.
[19] G. Deokar, P. Vancsó, R. Arenal, F. Ravaux, J. Casanova-Cháfer, E. Llobet, et al., MoS_2–carbon nanotube hybrid material growth and gas sensing, Adv. Mater. Interfaces 4 (2017), 1700801.
[20] H. Long, A. Harley-Trochimczyk, T. Pham, Z. Tang, T. Shi, A. Zettl, et al., High surface area MoS_2/graphene hybrid aerogel for ultrasensitive NO_2 detection, Adv. Funct. Mater. 26 (2016) 5158–5165.
[21] R. Kumar, N. Goel, M. Kumar, UV-activated MoS_2 based fast and reversible NO_2 sensor at room temperature, ACS Sens. 2 (2017) 1744–1752.
[22] T. Pham, G. Li, E. Bekyarova, M.E. Itkis, A. Mulchandani, MoS_2-based optoelectronic gas sensor with sub-parts-per-billion limit of NO_2 gas detection, ACS Nano 13 (2019) 3196–3205.
[23] Q. He, Z. Zeng, Z. Yin, H. Li, S. Wu, X. Huang, et al., Fabrication of flexible MoS_2 thin-film transistor arrays for practical gas-sensing applications, Small 8 (2012) 2994–2999.
[24] R. Kumar, N. Goel, M. Kumar, High performance NO_2 sensor using MoS_2 nanowires network, Appl. Phys. Lett. 112 (2018), 053502.
[25] D. Wu, Z. Lou, Y. Wang, T. Xu, Z. Shi, J. Xu, et al., Construction of MoS_2/Si nanowire array heterojunction for ultrahigh-sensitivity gas sensor, Nanotechnology 28 (2017), 435503.
[26] D. Sarkar, X. Xie, J. Kang, H. Zhang, W. Liu, J. Navarrete, et al., Functionalization of transition metal dichalcogenides with metallic nanoparticles: implications for doping and gas-sensing, Nano Lett. 15 (2015) 2852–2862.
[27] B. Cho, J. Yoon, S.K. Lim, A.R. Kim, S.-Y. Choi, D.-H. Kim, et al., Metal decoration effects on the gas-sensing properties of 2D hybrid-structures on flexible substrates, Sensors 15 (2015) 24903–24913.
[28] Y. Zhou, C. Gao, Y. Guo, UV assisted ultrasensitive trace NO_2 gas sensing based on few-layer MoS_2 nanosheet–ZnO nanowire heterojunctions at room temperature, J. Mater. Chem. A Mater. Energy Sustain. 6 (2018) 10286–10296.
[29] J.M. Suh, Y.-S. Shim, K.C. Kwon, J.-M. Jeon, T.H. Lee, M. Shokouhimehr, et al., Pd-and Au-decorated MoS_2 gas sensors for enhanced selectivity, Electron Mater Lett 15 (2019) 368–376.
[30] J. Guo, R. Wen, J. Zhai, Z.L. Wang, Enhanced NO_2 gas sensing of a single-layer MoS_2 by photogating and piezo-phototronic effects, Sci Bull 64 (2019) 128–135.
[31] W. Zheng, Y. Xu, L. Zheng, C. Yang, N. Pinna, X. Liu, et al., MoS_2 Van Der Waals p–n junctions enabling highly selective room-temperature NO_2 sensor, Adv. Funct. Mater. (2020), 2000435.
[32] C.R. Dean, A.F. Young, I. Meric, C. Lee, L. Wang, S. Sorgenfrei, et al., Boron nitride substrates for high-quality graphene electronics, Nat. Nanotechnol. 5 (2010) 722–726.
[33] A.V. Kretinin, Y. Cao, J.S. Tu, G.L. Yu, R. Jalil, K.S. Novoselov, et al., Electronic properties of graphene encapsulated with different two-dimensional atomic crystals, Nano Lett. 14 (2014) 3270–3276.
[34] Y.Y. Illarionov, G. Rzepa, M. Waltl, T. Knobloch, A. Grill, M.M. Furchi, et al., The role of charge trapping in MoS_2/SiO_2 and MoS_2/hBN field-effect transistors, 2d Mater. 3 (2016), 035004.
[35] D.H. Tien, J.-Y. Park, K.B. Kim, N. Lee, T. Choi, P. Kim, et al., Study of graphene-based 2D-heterostructure device fabricated by all-dry transfer process, ACS Appl. Mater. Interfaces 8 (2016) 3072–3078.
[36] A.N. Abbas, B. Liu, L. Chen, Y. Ma, S. Cong, N. Aroonyadet, et al., Black phosphorus gas sensors, ACS Nano 9 (2015) 5618–5624.
[37] N.M. Vuong, D. Kim, H. Kim, Surface gas sensing kinetics of a WO_3 nanowire sensor: part 1—oxidizing gases, Sensors Actuators B: Chem 220 (2015) 932–941.
[38] Y.W. Chang, J.S. Oh, S.H. Yoo, H.H. Choi, K.-H. Yoo, Electrically refreshable carbon-nanotube-based gas sensors, Nanotechnology 18 (2007), 435504.
[39] H. Choi, J.S. Choi, J.-S. Kim, J.-H. Choe, K.H. Chung, J.-W. Shin, et al., Flexible and transparent gas molecule sensor integrated with sensing and heating graphene layers, Small 10 (2014) 3685–3691.
[40] M. Donarelli, S. Prezioso, F. Perrozzi, F. Bisti, M. Nardone, L. Giancaterini, et al., Response to NO_2 and other gases of resistive chemically exfoliated MoS_2-based gas sensors, Sen. Actuators B: Chem 207 (2015) 602–613.
[41] R. Kumar, P.K. Kulriya, M. Mishra, F. Singh, G. Gupta, M. Kumar, Highly selective and reversible NO_2 gas sensor using vertically aligned MoS_2 flake networks, Nanotechnology 29 (2018), 464001.
[42] Y. Kang, S. Pyo, E. Jo, J. Kim, Light-assisted recovery of reacted MoS_2 for reversible NO_2 sensing at room temperature, Nanotechnology 30 (2019), 355504.
[43] G. Liu, S.L. Rumyantsev, C. Jiang, M.S. Shur, A.A. Balandin, Selective gas sensing with *h*-BN capped MoS_2 heterostructure thin-film transistors, IEEE Electron Device Lett 36 (2015) 1202–1204.
[44] N. Liu, J. Baek, S.M. Kim, S. Hong, Y.K. Hong, Y.S. Kim, et al., Improving the stability of high-performance multilayer MoS_2 field-effect transistors, ACS Appl. Mater. Interfaces 9 (2017) 42943–42950.
[45] Y. Li, C.-Y. Xu, L. Zhen, Surface potential and interlayer screening effects of few-layer MoS_2 nanoflakes, Appl. Phys. Lett. 102 (2013), 143110.

Biographies

Dr. Ayaz Ali received his BS degree in Electronics from University of Sindh, Jamshoro, in 2009, MS and PhD degree in Microelectronics from Zhejiang University, China in 2014 and 2018 respectively. Currently, he is a postdoc fellow at SINTEF, Oslo. His research interest focuses on CMOS integration of graphene like 2D materials (BN, BP and TMDs) for high-performance heterostructure devices such as broadband photodetectors and emerging smart sensors for the internet-of things and flexible electronics.

Dr. Ozhan Koybasi is a Senior Scientist at SINTEF in the department of Microsystems and Nanotechnology. He obtained his MS degree in 2010 and PhD degree in 2011 from Purdue University in electrical engineering and physics, respectively. He joined SINTEF in 2013, and since then, he has been leading R&D and production projects on semiconductor-based radiation detectors and photodetectors. His other research interests include application of 2D materials and related materials in different types of sensors such as gas sensors and photodetectors.

Dr. Wen Xing currently works as research scientist at the Department of Thin Film and Membrane Technology, SINTEF. He obtained his PhD in 2013 at University of Oslo, Norway. His current research interests are electrochemistry in high temperature energy converting materials, gas separation membranes and 2D materials.

Dr. Daniel Nilsen Wright received his MChem in chemical physics from Liverpool University in 2001 and his PhD in physics from the University of Oslo in 2008. He is currently a research scientist at SINTEF working as a project leader for projects involving silicon device fabrication and advanced electronic packaging.

Dr. Deepak Varandani is a Senior Scientist in Thin Film Laboratory, Department of Physics, Indian Institute of Technology Delhi. His current research interests are synthesis and characterization of nanomaterials.

Dr. Takashi Taniguchi is Researcher in the National Institute for Materials Science, Japan. His current research interests are synthesis, optical and electrical characterization of novel 2D materials.

Dr. Kenji Watanabe is Researcher in the National Institute for Materials Science, Japan. His current research interests are synthesis, optical and electrical characterization of novel 2D materials.

Prof. Bodh R. Mehta is currently Dean (R&D), Schlumberger Chair Professor and member of technical committee on sensor based ambient air monitoring systems (Central Pollution Control Board, India). He leads a group which has extensive experience in the field of thin film and nanomaterials for gas sensing, Solar Cell, Resistive Memory, Thermoelectric and photoelectrochemical applications.

Dr. Branson Belle is a Senior Scientist at SINTEF in the department of Renewable Energy Technology. He obtained his PhD in 2007 from the University of Manchester in the field of Magnetism. His current research interests are the development of sensors and devices based on 2D material heterostructures as well as atomic force microscopy.